Differential vesicular sorting of AMPA and GABAA receptors

Yi Gu[a,1], Shu-Ling Chiu[a,2], Bian Liu[a,2], Pei-Hsun Wu[b,2], Michael Delannoy[c], Da-Ting Lin[a,3], Denis Wirtz[b], and Richard L. Huganir[a,4]

[a]Department of Neuroscience, Johns Hopkins University School of Medicine, Baltimore, MD 21205; [b]Department of Chemical and Biomolecular Engineering, Johns Hopkins University, Baltimore, MD 21218; and [c]Johns Hopkins University School of Medicine Microscope Facility, Baltimore, MD 21205

In mature neurons AMPA receptors cluster at excitatory synapses primarily on dendritic spines, whereas GABAA receptors cluster at inhibitory synapses mainly on the soma and dendritic shafts. The molecular mechanisms underlying the precise sorting of these receptors remain unclear. By directly studying the constitutive exocytic vesicles of AMPA and GABAA receptors in vitro and in vivo, we demonstrate that they are initially sorted into different vesicles in the Golgi apparatus and inserted into distinct domains of the plasma membrane. These insertions are dependent on distinct Rab GTPases and SNARE complexes. The insertion of AMPA receptors requires SNAP25–syntaxin1A/B–VAMP2 complexes, whereas insertion of GABAA receptors relies on SNAP23–syntaxin1A/B–VAMP2 complexes. These SNARE complexes affect surface targeting of AMPA or GABAA receptors and synaptic transmission. Our studies reveal vesicular sorting mechanisms controlling the constitutive exocytosis of AMPA and GABAA receptors, which are critical for the regulation of excitatory and inhibitory responses in neurons.

AMPA receptor | GABAA receptor | constitutive exocytosis | TIRFM | SNARE

In the mammalian central nervous system, neurons receive excitatory and inhibitory signals at synapses. Specific receptors at postsynaptic membranes are activated by neurotransmitters released by presynaptic terminals. Most fast excitatory neurotransmission is mediated by AMPA receptors, the majority of which are heterotetramers of GluA1/GluA2 or GluA2/GluA3 subunits in the hippocampus (1). Fast synaptic inhibition is largely mediated by GABAA receptors, which are predominantly heteropentamers of two α subunits, two β subunits, and one γ or δ subunit in the hippocampus (2). Numerous studies have demonstrated AMPA receptors are selectively localized at excitatory synapses on dendritic spines, whereas GABAA receptors cluster at inhibitory synapses localized on dendritic shafts and the soma (3). This segregation of excitatory and inhibitory receptors requires highly precise sorting machinery to target receptors to distinct synapses opposing specific presynaptic terminals. However, it is still not clear whether the receptors are sorted before exocytosis into the plasma membrane or are differentially localized only after exocytosis. For example in a "plasma membrane sorting model," different receptors could be pooled into the same vesicle and inserted along the somatodendritic membrane. The initial sorting would occur on the plasma membrane, where inserted receptors would be segregated by lateral diffusion and stabilization at different postsynaptic zones. Alternatively, in a "vesicle sorting model," different receptors would first be sorted into different vesicles during intracellular trafficking processes and independently inserted to the plasma membrane, where receptors could be further targeted to specific zones and stabilized by synaptic scaffolds. To date there has been no direct evidence to support either model. However, a large body of literature suggests that the exocytic pathways of AMPA and GABAA receptors have similar but also distinct properties (1, 2).

Increasing evidence has suggested roles for the SNARE protein family in vesicular trafficking of AMPA and GABAA receptors (4–17). SNAREs are a large family of membrane-associated proteins

critical for many intracellular membrane trafficking events. The family is subdivided into v-SNAREs (synaptobrevin/VAMP, vesicle-associated membrane proteins) and t-SNAREs (syntaxins and SNAP25, synaptosomal-associated protein of 25 kDa) based on their localization on trafficking vesicles or target membranes, respectively. To mediate vesicle fusion with target membranes, SNARE proteins form a four-helix bundle (SNARE complex) consisting of two coiled-coil domains from SNAP25, one coiled-coil domain from syntaxin, and a coiled-coil domain from VAMPs (18). Formation of the helical bundle can be disrupted by neurotoxins, which specifically cleave different SNARE proteins (19). Each SNARE subfamily is composed of genes with high homology but different tissue specificity and subcellular localization. It remains to be determined whether individual SNAREs play specific roles in regulating the membrane trafficking of individual proteins.

To address how AMPA and GABAA receptors are sorted in the exocytic pathway and what molecules are involved in regulating exocytosis of these receptors, we specifically studied constitutive exocytosis of AMPA and GABAA receptor subunits using total internal reflection fluorescence microscopy (TIRFM) in combination with immunocytochemistry, electrophysiology, and electron microscopy methods. Together, we revealed that AMPA and GABAA receptors are initially sorted into different vesicles in the Golgi apparatus and delivered to different domains at the plasma membrane and are regulated by specific Rab proteins and

Significance

In neurons most fast excitatory neurotransmission is mediated by AMPA receptors, which cluster at excitatory synapses primarily on dendritic spines. Fast synaptic inhibition is largely mediated by GABAA receptors, which cluster at inhibitory synapses mainly on the soma and dendritic shafts. It is unclear how these receptors are segregated and delivered to specific locations on the plasma membranes. Here we directly studied the constitutive exocytosis of AMPA and GABAA receptors and demonstrate that they are initially sorted into different vesicles in the Golgi apparatus and inserted into distinct domains of the plasma membrane. Their exocytosis is dependent on distinct Rab GTPases and SNARE complexes. Our results reveal fundamental mechanisms underlying the sorting of excitatory and inhibitory neurotransmitter receptors in neurons.

SNARE complexes. These results reveal fundamental mechanisms underlying the sorting of excitatory and inhibitory neurotransmitter receptors in neurons and uncover the specific trafficking machinery involved in the constitutive exocytosis of each receptor type.

Results

Dynamic Events of AMPA and GABA$_A$ Receptors on the Plasma Membrane of Hippocampal Pyramidal Neurons.

To visualize individual exocytosis events of AMPA or GABA$_A$ receptors in living hippocampal neurons, we used TIRFM to specifically image trafficking events at or immediately beneath the plasma membrane in contact with the coverslip (100–200 nm) (20). To further ensure the imaging of exocytic events, supercliptic pHluorin (pHluorin or pH) was chosen to tag the extracellular N terminus of AMPA and GABA$_A$ receptors. pHluorin is an EGFP variant that fluorescences brightly at pH 7.4 and is fully quenched in the lumen of secretory organelles having a pH <6 (21). Therefore, after exocytosis the fluorescent signal of pHluorin-tagged receptors dramatically increases under the exposure of imaging solution with pH 7.4 (14, 15, 22). pHluorin-tagged GluA2 (pH-GluA2) and γ2S (pH-γ2S) were used for the study, because these subunits are common subunits of AMPA and GABA$_A$ receptor complexes in hippocampus, respectively. Previous studies have confirmed that the pHluorin tag does not affect trafficking of these receptor subunits in neurons (15, 23).

pHluorin-tagged GluA2 or γ2S was expressed in dissociated hippocampal neurons and directly visualized under TIRFM. Before recording, the entire cell surface in the TIRF field was photobleached to eliminate signals from preexisting surface receptors and isolate new exocytic events (22). We observed robust dynamic events of pH-GluA2 and pH-γ2S throughout the plasma membranes. Most events of GluA2 and γ2S occurred on the extrasynaptic membrane in the cell body and dendritic shafts (Fig. 1A and Movies S1 and S2). We did not observe events of pH-GluA2 on dendritic spines. These dynamic events transiently

occurred at high frequency: 95.8% events of pH-GluA2 lasted less than 7 s with the main duration around 2.8 s, whereas 96.7% events of pH-γ2S lasted less than 7 s with main duration around 2.1 s (Fig. 1 B and C). The mean event duration of pH-GluA2 was significantly longer than that of pH-γ2S (Fig. S1A). There are 22 ± 2 events per second per 100 μm^2 for pH-γ2S and 15 ± 1 events per second per 100 μm^2 for pH-GluA2. These frequencies remained stable under imaging with higher frame rate (Fig. S1B). To confirm that these dynamic events are on the plasma membrane we performed an acidification–neutralization test (24), which included 15–30 s of TIRF imaging in pH 7.4 extracellular solution, then a fast perfusion for 15–30 s with pH 5.5 extracellular solution, followed by a return to pH 7.4 extracellular solution. Most of dynamic events of pH-GluA2 and pH-γ2S quenched upon acidic perfusion and recovered immediately after reneutralization (Fig. 1D and Fig. S1C). In addition, when neurons were perfused with the pH 7.4 solution containing ammonium chloride (NH$_4$Cl), which rapidly alkalinized all of the acidic intracellular pools and revealed intracellular pH receptors (21), the frequency of the dynamic TIRF events remained constant. These results strongly suggest that the dynamic events under TIRFM present on the plasma membrane. Moreover, the frequency of these events was not regulated by neuronal activity, which was acutely suppressed or enhanced by brief application of TTX or KCl, respectively (Fig. S1D), suggesting these are constitutive trafficking events. Overall, these results indicate that the transient extrasynaptic events of GluA2 and γ2S under TIRFM are constitutive dynamics of receptors on the plasma membrane.

We noticed that most of the events of GluA2 and γ2S have dim fluorescence intensity, suggesting that each event contains a low number of receptor subunits. To confirm this observation, we measured the number of fluorescent receptors per event (22). Based on the knowledge that the fluorescent intensity of the EGFP monomer is similar to the intensity of pHluorin in the environment of pH 7.4 (24), we compared the fluorescent intensity
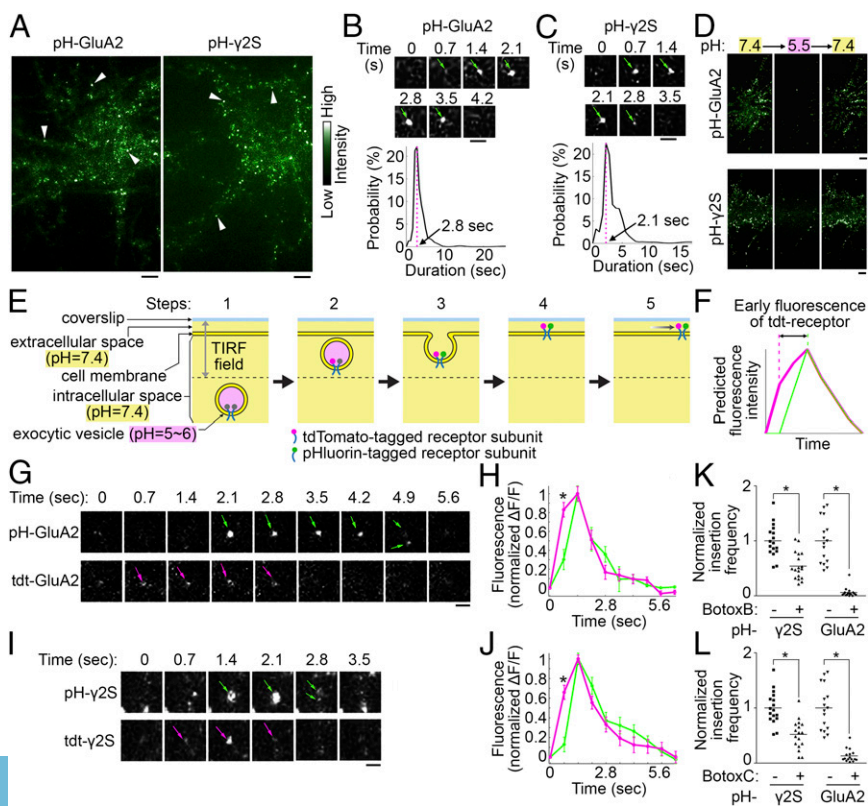

Fig. 1. Exocytic events of pH-GluA2 and pH-γ2S under TIRFM. (A) Dynamic TIRF events of pH-GluA2 and pH-γ2S are highlighted based on intensity. Typical events are indicated by white arrowheads. Imaging frequency is 1.4 Hz with 500-ms exposure. (Scale bars: 5 μm.) (B and C) Dynamic events of pH-GluA2 (B) and pH-γ2S (C) are transient. (Top) Time series of a single event. (Bottom) Distribution of event durations. Arrows indicate the main event duration. n = 120 for both receptors. (Scale bars: 1 μm.) (D) Acidification–neutralization analysis of pH-GluA2 and pH-γ2S events. From left to right: cells in the extracellular solution at pH 7.4, 5.5, and 7.4. (Scale bars: 5 μm.) (E) Dynamics of an exocytic vesicle containing two receptor subunits differentially tagged with pHluorin and tdTomato. (F) Predicted dynamics of tdTomato and pHluorin receptors in the same exocytic vesicle under TIRFM. (G and I) TIRF dynamics of a coinsertion vesicle containing tdt-GluA2 and pH-GluA2 (G) or tdt-γ2S and pH-γ2S (I). (Scale bars: 1 μm.) (H and J) Time course of tdt-GluA2 and pH-GluA2 (H) or tdt-γ2S and pH-γ2S (J) from multiple coinsertion events. In H, n = 27; in J, n = 31. (K and L) Dynamic events of GluA2 and γ2S are inhibited by Botox B (K) or Botox C (L). The same control dataset was used. Each data point is one cell. The line in each dataset shows mean frequency. Event frequencies of all cells were normalized by the mean of the control. Asterisks indicate statistical significances.

www.manaraa.com

of EGFP monomer to the intensity of single events of pH-GluA2 and pH-γ2S under TIRFM. EGFP monomers were confirmed by their blinking dynamics and single-step photobleaching property (22) (Fig. S1E). The intensity of EGFP monomers, pH-GluA2–containing vesicles, and pH-γ2S–containing vesicles follows Gaussian distributions (Fig. S1 F–H). The peak intensities of fitted Gaussian curves for EGFP monomers, pH-GluA2, and pH-γ2S events indicate that each pH-GluA2 event contains on average two pH-GluA2 subunits (2.2 ± 0.1 subunits per event), whereas each pH-γ2S event contains around four pH-γ2S subunits (3.9 ± 0.2 subunits per event). We and others have previously characterized larger, much less frequent GluA2 and GluA1 insertion events that have slower kinetics and are distinct from these rapid insertion events (14, 15, 22). Because of the much lower frequency of these larger events (two to six insertions per minute) they did not significantly contribute to the quantitation and characterization of the smaller events.

Dynamic TIRF Events of GluA2 and γ2S Are Exocytic Events. Several lines of evidence suggest that the dynamic surface events of GluA2 and γ2S under TIRFM are exocytic events. First, the exocytic feature is supported by the stereotypic dynamics of these events under TIRFM. As demonstrated in Fig. 1E, when two subunits of the same receptor differentially tagged with pHluorin and a red fluorescent protein (pH-insensitive; for example, tdTomato) and delivered in the same exocytic vesicle (coinsertion), they exhibit different dynamics under TIRFM. The pH-insensitive red fluorescent protein is excited immediately when the exocytic vesicle enters the TIRF field. However, pHluorin remains quenched until it is exposed to the extracellular space (pH 7.4) after the exocytosis. Therefore, the red fluorescence increases in advance of the green fluorescence (Fig. 1F).

To investigate whether the events of GluA2 and γ2S also exhibit this stereotypic dynamics of exocytosis under TIRF, we first tagged GluA2 and γ2S with pH-insensitive red fluorescent protein tdTomato and characterized the tagged receptor subunits (Fig. S2). In live hippocampal neurons tdt-GluA2 or tdt-γ2S colocalized with EGFP-GluA2 or EGFP-γ2S, respectively (Fig. S2 A and D). In addition, tdt-GluA2 (Fig. S2 B and C) and tdt-γ2S (Fig. S2 E and F) also colocalized well with endogenous GluA1 and β2/3, respectively, indicating that these tdTomato-tagged receptors trafficked similarly to endogenous receptors. Moreover, tdt-GluA2 and tdt-γ2S could be stained in live cells with anti-tdTomato antibody, indicating that these receptors were expressed on the surface (Figs. S3 and S4). Total and surface tdt-GluA2 colocalized with the excitatory postsynaptic marker PSD95 (postsynaptic density protein 95) (Fig. S3 A and B) and the presynaptic marker VGluT (vesicular glutamate transporter) (Fig. S3 C and D). Similarly, total and surface tdt-γ2S colocalized with the inhibitory postsynaptic marker gephyrin (Fig. S4 A and B) and the presynaptic marker VGAT (vesicular GABA transporter) (Fig. S4 C and D). These data suggest that tdTomato-tagged GluA2 and γ2S are properly trafficked and targeted in hippocampal neurons.

We then coexpressed pH receptor and tdt receptor and simultaneously visualized their exocytosis under dual-color TIRFM with 488-nm and 568-nm lasers to excite green and red fluorescent proteins, respectively. Dynamics of events containing both green and red fluorescence signals (coinsertion events) were analyzed. As expected, in the coinsertion events of pH-GluA2 and tdt-GluA2, the fluorescence of tdt-GluA2 increased earlier than that of pH-GluA2 (Fig. 1 G and H). Similar dynamics was also observed in the coinsertion events of pH-γ2S and tdt-γ2S (Fig. 1 I and J). The particular dynamics of these coinsertions under TIRF strongly suggest that they are exocytic events. In many events, we also observed that the fluorescence of tdTomato receptor decayed faster than the pHluorin fluorescence. This phenomenon is likely caused by the photoinstability of tdTomato compared to pHluorin (26).

The second evidence of exocytosis is based on the results of botulinum toxin (Botox) treatments. Receptor exocytosis occurs when an intracellular vesicle, which carries assembled receptor complexes, fuses to the plasma membrane and the receptor complexes are delivered to the plasma membrane (27). This process highly depends on SNARE proteins, which can be cleaved by different Botoxs (19). Therefore, we tested the effects of Botoxs on the TIRF event frequencies of pH-GluA2 and pH-γ2S. Botox B, which cleaves VAMP2 (Fig. S5 C and D), reduced frequency of both GluA2 and γ2S events (Fig. 1K). Similarly, Botox C, which cleaves rat SNAP25, syntaxin1A, 1B, 2, and 3 (Fig. S5 E–J), inhibited events of GluA2 and γ2S (Fig. 1L). Notably, we detected a low degree of the incomplete blockade of exocytic events, which was commonly reported with botulinum toxin treatments. This is likely due to the inability of Botoxs to proteolyze SNARE proteins in assembled complexes (Fig. S5) (28).

Finally, we also observed receptor dispersion to the surrounding regions after exocytosis, which is another stereotypic dynamic of exocytic events (14). As shown in Fig. S6, pH-GluA2 events showed increased fluorescence in the surrounding region while the fluorescence in the insertion spot decayed (Fig. S6 A and B). The appearance of fluorescence peak in the surrounding region was significantly delayed in comparison with the one in the insertion center, strongly indicating the receptor dispersion after the insertion (Fig. S6 C and D). A similar phenomenon was observed for pH-γ2S events (Fig. S6 E–H). In addition, many events showed the separation of receptor subunits during this dispersion process (Fig. S6 A and E), suggesting that each inserted receptor complex can diffuse independently.

In summary, the Botox sensitivity and stereotypic dynamics of these events under TIRFM strongly suggest that they are exocytic events of GluA2 and γ2S.

Exocytosis of AMPA and GABA_A Receptors Is Mediated by Different SNAPs. Although Botox B and C inhibited exocyosis of both GluA2 and γ2S, Botox A, which cleaves SNAP25 (Fig. S5 A and B), showed different effects on exocytosis of pH-GluA2 and pH-γ2S. As shown in Fig. 2A, Botox A inhibited exocytosis of GluA2, but not γ2S. These Botox-treatment results indicate that exocytosis of both AMPA and GABA_A receptors require VAMP2 and syntaxins, but the different receptors likely require different SNAPs: SNAP25 mediates AMPA receptor insertion, whereas a Botox A-insensitive SNAP mediates GABA_A receptor insertion.

Three Botox A-insensitive SNAPs (SNAP23, SNAP29, and SNAP47) are expressed in rat hippocampal neurons (29). All three SNAPs are known to regulate membrane fusion events in neurons (13, 16, 17, 30–32). We examined the effect of shRNAs that specifically knock down each SNAP (Fig. S7 A–E) on the exocytosis frequencies of AMPA and GABA_A receptors, compared with a control shRNA with a sequence not targeting any known vertebrate genes. Consistent with Botox A treatment, SNAP25 knockdown reduced the frequency of exocytosis of GluA2, but not γ2S, and this inhibition was fully rescued by shRNA-resistant SNAP25 but not SNAP23 (Fig. 2B). However, knockdown of SNAP23 blocked exocytosis of γ2S, but not GluA2, and this effect was rescued by shRNA-resistant SNAP23 but not SNAP25 (Fig. 2C). The effects of SNAP25 and SNAP23 shRNAs were observed on both somatic and dendritic exocytosis of pH-GluA2 and pH-γ2S (Fig. S7 J–M). Knockdown of SNAP29 or SNAP47 did not significantly affect exocytosis of either GluA2 or γ2S (Fig. S7 N and O). These results demonstrated that SNAP25 and SNAP23 specifically mediate the constitutive exocytosis of GluA2- and γ2S-containing receptors, respectively.

If SNAP25 and SNAP23 knockdown reduced constitutive exocytosis of AMPA and GABA_A receptors, respectively, we would predict that this would decrease the surface expression of these receptors. To test this possibility, we examined surface levels of endogenous GluA2 and γ2 by immunostaining of surface receptors
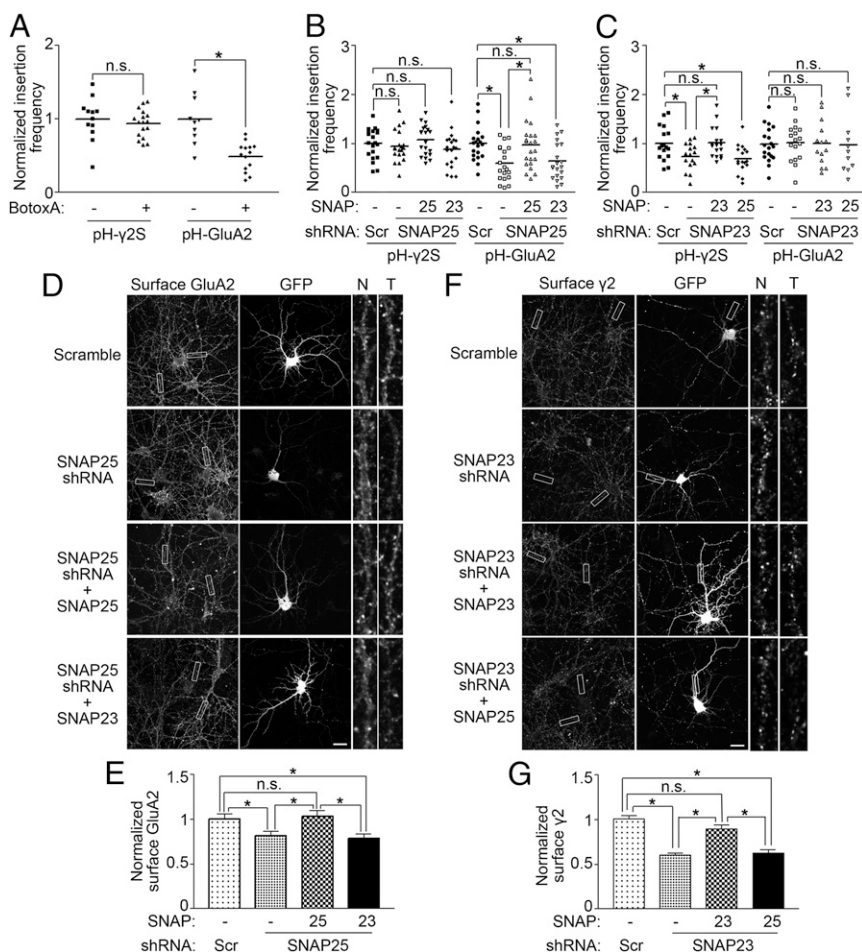
Fig. 2. Exocytic events of GluA2 and γ2S are constitutive events mediated by different SNAPs. (*A*) Insertion of GluA2 and γ2S are differently affected by Botox A treatment. (*B*) SNAP25 is required for insertions of GluA2, but not γ2S. Scramble shRNA (Scr), SNAP25 shRNA, shRNA-resistant SNAP25 (25), or SNAP23 (23) were coexpressed with pH-receptors for 24 h. (*C*) SNAP23 is required for insertions of γ2S, but not GluA2. Scramble shRNA (Scr), SNAP23 shRNA, shRNA-resistant SNAP23 (23), or SNAP25 (25) were coexpressed with pH-receptors for 48 h. (*D*) Knockdown of SNAP25 reduces endogenous surface GluA2. SNAP25 shRNA, shRNA-resistant SNAP25 (SNAP25), or SNAP23 were coexpressed with EGFP to label transfected hippocampal neurons for 72 h. Right panels: high-magnification images of the individual processes boxed in left panels. N, surface GluA2 in nontransfected neurons; T, surface GluA2 in transfected neurons. (Scale bar: 20 μm.) (*E*) Quantification of surface GluA2 in *D*. Relative surface GluA2 in transfected neurons is represented by a ratio of surface GluA2 in transfected cells to that of nontransfected cells. The ratios were normalized by the average of the control transfected with the scramble shRNA. Scr: scramble shRNA. 25: shRNA-resistant SNAP25. 23: SNAP23. *n* = 18–22 neurons for each group. Five processes were selected in each neuron. (*F*) Knockdown of SNAP23 reduces endogenous surface γ2. SNAP23 shRNA, shRNA-resistant SNAP23 (SNAP23), or SNAP25 were coexpressed with EGFP to label transfected cells for 72 h. (Scale bar: 20 μm.) (*G*) Quantification of surface γ2 in *F* was performed similarly as in *E*. Scr: scramble shRNA. 23: shRNA-resistant SNAP23. 25: SNAP25. *n* = 25–30 neurons for each group. Five processes were selected in each neuron. Asterisks indicate statistical significances. n.s., no statistical significance.

while the SNAPs were specifically knocked down. Indeed, SNAP25 shRNA significantly reduced surface GluA2 levels in hippocampal neurons. This effect was rescued by shRNA-resistant SNAP25 but not SNAP23 (Fig. 2 *D* and *E*). Conversely, SNAP23 shRNA drastically reduced surface γ2 levels, which was rescued by shRNA-resistant SNAP23 but not SNAP25 (Fig. 2 *F* and *G*). However, knockdown of SNAP23 or SNAP25 did not affect surface levels of GluA2 or γ2, respectively (Fig. S8).

We then asked whether SNAP25 and SNAP23 regulate surface expression of endogenous GluA2 and γ2 subunits at synapses, respectively. In hippocampal neurons knockdown of SNAP25, rather than SNAP23, reduced synaptic surface GluA2, which colocalized with the excitatory presynaptic marker VGluT (Fig. 3 *A* and *B*). However, knockdown of SNAP23, but not SNAP25, significantly reduced synaptic surface levels of γ2, which colocalized with the inhibitory presynaptic marker VGAT (Fig. 3 *C* and *D*). Given our observations that most insertions of GluA2 and γ2S occur at extrasynaptic sites (Movies S1 and S2), these reductions in synaptic surface GluA2 and γ2 could result from the depletion of extrasynaptic surface receptors, which supply synaptic receptor pools by lateral diffusion to the postsynaptic membrane. These data suggest that SNAP25 and SNAP23 regulate not only the surface expression of GluA2 and γ2 subunits throughout the entire neuron, but also specifically regulate the synaptic surface expression of GluA2 and γ2, respectively.

The reduced surface expressions of GluA2 and γ2 at synapses suggest that SNAP25 and SNAP23 may affect AMPA and GABA$_A$ receptor-mediated synaptic transmission. To test this hypothesis, whole-cell patch-clamp recording was used to examine AMPA receptor-mediated mEPSCs (miniature excitatory postsynaptic

currents) and GABA$_A$ receptor-mediated mIPSCs (miniature inhibitory postsynaptic currents) in hippocampal neurons with SNAP25 or SNAP23 knockdown by specific shRNAs. Strikingly, knockdown of SNAP25, but not SNAP23, preferentially reduced AMPA receptor-mediated mEPSC amplitude (Fig. 3 *E* and *F*), whereas knockdown of SNAP23, but not SNAP25, significantly reduced GABA$_A$-receptor mediated mIPSC amplitude (Fig. 3 *G* and *H*). These results are consistent with the specific effects of SNAP25 and SNAP23 on constitutive exocytosis and synaptic surface levels of GluA2 and γ2S, respectively. The SNAP25 or SNAP23-dependent exocytosis of AMPA or GABA$_A$ receptors significantly affects excitatory and inhibitory synaptic transmission in neurons at the basal state.

Overall, our results reveal important postsynaptic roles of SNAP25 and SNAP23 on constitutive insertions, surface expression of GluA2 and γ2, and basal synaptic transmission mediated by AMPA and GABA$_A$ receptors, respectively. The distinct functions of SNAP25 and SNAP23 support the model that AMPA and GABA$_A$ receptors are inserted into the plasma membrane via different vesicles that are under regulation of specific SNAPs.

Exocytosis of AMPA and GABA$_A$ Receptors Is Mediated by Syntaxin1 and VAMP2. We further investigated other SNARE components necessary for fusion of AMPA or GABA$_A$ receptor-containing vesicles to the plasma membrane. In rat hippocampal neurons, five syntaxins are expressed on the plasma membrane: syntaxin1A, syntaxin1B, syntaxin2, syntaxin3, and syntaxin4 (33). All syntaxins, except syntaxin4, can be cleaved by Botox C (Fig. S5 *E–J*) (34). SNAP25 and SNAP23 have higher affinities to syntaxin1A, 1B, and syntaxin4 than to syntaxin2 and 3 (35–37). We therefore

Gu et al.

Fig. 3. Effects of of SNAP25 and SNAP23 on synaptic surface expression of GluA2 and γ2S and basal synaptic transmission. (*A*) Knockdown of SNAP25, but not SNAP23, reduces the surface GluA2 at the excitatory postsynaptic membrane. Scramble, SNAP25, or SNAP23 shRNA were coexpressed with EGFP (to label transfected neurons) in hippocampal neurons for 72 h. (*Top*) Surface GluA2 (s-GluA2). (*Middle*) VGluT. (*Bottom*) White puncta showing colocalization of s-GluA2 (magenta) and VGluT (green). Synaptic surface GluA2 in shRNA-transfected cells (shRNA) was compared with nontransfected cells (–) on the same coverslip. Yellow arrows at the corresponding locations in all three panels indicate the s-GluA2, VGluT, and overlaid signals at the same synapse. (Scale bar: 10 μm.) (*B*) Quantification of the synaptic surface GluA2 in *A*. In each shRNA-transfected neuron, relative synaptic surface GluA2 was computed as a ratio of the surface synaptic GluA2 of transfected neurons to that of nontransfected neurons. The ratio in each sample was normalized by the average of the scramble shRNA control. Scr: scramble shRNA. 25: SNAP25 shRNA. 23: SNAP23 shRNA. $n = 18$–22 for shRNA-transfected neurons. Ten synapses were selected in each transfected neuron and nontransfected neurons. (*C*) Knockdown of SNAP23, but not SNAP25, reduces the surface γ2 at the inhibitory postsynaptic membrane. Scramble, SNAP23, or SNAP25 shRNA were coexpressed with EGFP (to label transfected neurons) for 72 h. (Scale bar: 10 μm.) (*D*) Quantification of the surface synaptic γ2 in *C* was performed similarly as in *B*. $n = 28$–30 for shRNA-transfected neurons. (*E* and *G*) Whole-cell recordings were performed on hippocampal neurons 3 d after transfection of scramble (Scr), SNAP25 (25), or SNAP23 shRNAs (23). Representative traces of spontaneous AMPA receptor-mediated mEPSCs and GABA_A receptor-mediated mIPSCs for each group are shown in *E* and *G*, respectively. (*F*) Quantification of AMPA mEPSC amplitudes in *E*. SNAP25-knockdown neurons have significantly smaller amplitudes than control (Mann–Whitney test, $P < 0.01$). Scramble shRNA = -18.2 ± 0.65 pA, SNAP25 shRNA = -15.1 ± 0.69 pA, SNAP23 shRNA = -17.2 ± 1.63 pA. $n = 11$–14 for each group. (*H*) Quantification of GABA_A mIPSC amplitudes in *G*. SNAP23 knockdown neurons have significantly smaller amplitudes than control (Mann–Whitney test, $P < 0.001$). Scramble shRNA = -55.8 ± 4.67 pA, SNAP23 shRNA = -31.8 ± 2.99 pA, SNAP25 shRNA = -51.3 ± 4.55 pA. $n = 10$–13 for each group. Asterisks indicate statistical significances. n.s., no statistical significance.
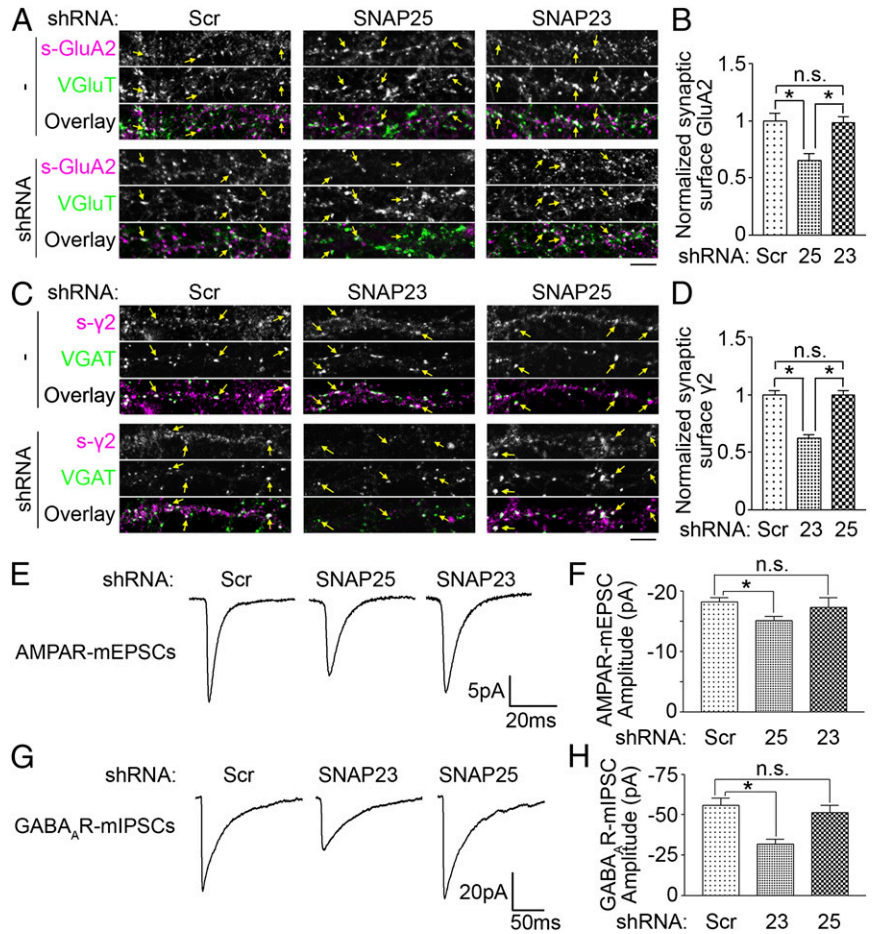
tested whether syntaxin1A, 1B, or syntaxin4 could be the t-SNAREs mediating exocytosis of GluA2 or γ2S. We used specific shRNAs to knock down these three syntaxins (Fig. S7 *F–H*) and examined the effect on exocytosis of GluA2 or γ2S. Knockdown of syntaxin1A and 1B significantly reduced exocytic frequencies of both GluA2 and γ2S. This effect could be rescued by shRNA-resistant syntaxin1A and 1B, respectively (Fig. 4 *A* and *B*). Knockdown of syntaxin4 did not affect exocytosis of either GluA2 or γ2S (Fig. S7*P*). In conclusion, the constitutive insertion of GluA2- or γ2S-containing vesicles into the plasma membrane is commonly mediated by two t-SNAREs: syntaxin1A and 1B.

There are two VAMPs, VAMP1 and VAMP2, specifically expressed in the rat brain, including hippocampus (38–40). To test which VAMPs are important for pH-GluA2 and pH-γ2S exocytosis, we used shRNAs to specifically knock down VAMP1 and VAMP2 (Fig. S7*I*) and investigated their effects on the exocytosis of GluA2 and γ2S. Consistent with our previous observation that Botox B, which cleaves VAMP2, reduced the exocytic frequency of both pH-GluA2 and pH-γ2S (Fig. 1*K*), depletion of VAMP2 significantly reduced exocytic frequencies of both pH-GluA2 and pH-γ2S (Fig. 4*C*). However, knockdown of VAMP1, which is not cleaved by Botox B, had no effect on exocytosis of either pH-GluA2 or pH-γ2S (Fig. S7*Q*). Together, these results demonstrate that VAMP2, but not VAMP1, serves as a v-SNARE mediating the constitutive exocytosis of both GluA2- and γ2S-containing AMPA and GABA_A receptors.

Exocytosis of AMPA and GABA_A Receptors Is Differentially Regulated by Specific Rab Proteins. Surface receptors can be delivered to the plasma membrane along different trafficking pathways, such as the de novo exocytic pathway originating from Golgi apparatus and recycling pathways involving early and recycling endosomes. These exocytic pathways are regulated by the small GTPase Rab protein family (41). To investigate the source of the receptor-containing vesicles, we coexpressed pHluorin-tagged receptors with dominant negative Rab proteins that interfere with specific trafficking pathways. A dominant negative Rab8 [Rab8(T22N)], which blocks vesicle trafficking from the Golgi apparatus to the plasma membrane (de novo exocytosis), reduced the exocytic frequency of both GluA2 and γ2S (Fig. 4*D*). Dominant negative Rab4, 5, and 11 [Rab4(S22N), Rab5(S34N), and Rab11(S25N)], which block different steps in the vesicle recycling pathway including sorting from early endosomes to the plasma membrane, endocytosis, and trafficking from recycling endosomes to the plasma membrane, only significantly inhibited exocytosis of GluA2, but not γ2S (Fig. 4 *E–G*). These results suggest that constitutive exocytic events of GluA2 include both de novo exocytic and recycling events, whereas constitutive exocytic events of γ2S are mostly de novo exocytic events.

Exocytosis of AMPA and GABA_A Receptors Targets Different Zones on the Plasma Membrane. Exocytic events of pH-GluA2 and pH-γ2S not only occurred under different molecular mechanisms, but also show distinct spatial targeting on the plasma membrane.
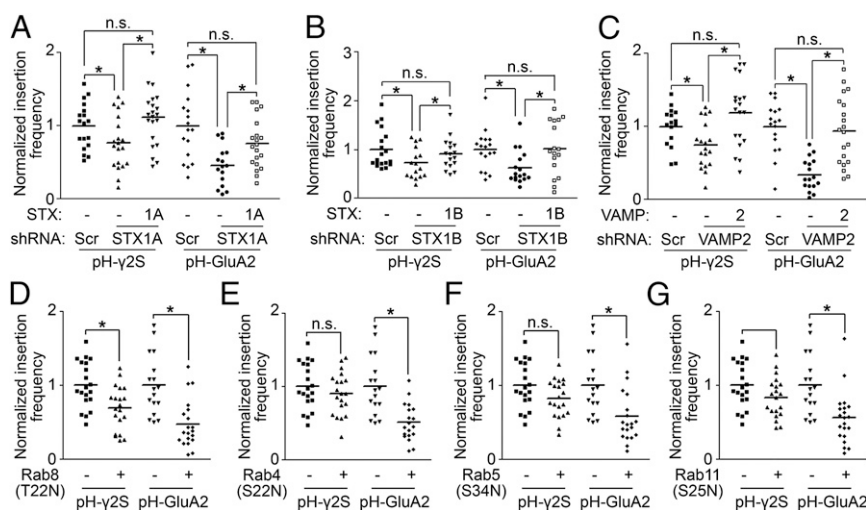
Fig. 4. Syntaxin1, VAMP2, and specific Rab proteins regulate exocytosis of GluA2 and γ2S. (A–C) Syntaxin1A (A), syntaxin1B (B), and VAMP2 (C) are required for exocytosis of γ2S and GluA2. Scramble shRNA (Scr), syntaxin1A (STX1A), syntaxin1B (STX1B), or VAMP2 shRNA (VAMP2) and shRNA-resistant syntaxin1A (1A), syntaxin1B (1B), or VAMP2 (2) were coexpressed with pH receptors for 48 h. (D–G) Effects of dominant negative Rabs on exocytosis of GluA2 and γ2S. Rab8(T22N) (D), Rab4(S22N) (E), Rab5(S34N) (F), Rab11(S25N) (G), or empty vector was coexpressed with pH receptors for 24 h. The same empty vector control was used in D–G. Asterisks indicate statistical significances. n.s., no statistical significance.

Using an intensity-based program, exocytic events of pH-GluA2 and pH-γ2S were automatically isolated (Fig. S9A). Strikingly, we found that the pH-GluA2 exocytic events occur in the central region of the plasma membrane in contact with the coverslip, whereas the pH-γ2S exocytic events distribute in the peripheral region of the plasma membrane (Fig. 5A and Movies S3 and S4).

To confirm the spatial segregation of exocytosis of pH-GluA2 and pH-γ2S, we coexpressed GluA2 or γ2S tagged with tdTomato or pHluorin in the same cell and simultaneously visualized their exocytic events using dual-color TIRFM. Consistent with the previous observations, exocytic events of pH-γ2S and tdt-GluA2 have different distributions on the somatic plasma membrane in contact with the coverslip. Vesicles containing pH-γ2S are mainly targeted to the outer peripheral region of the soma, whereas tdt-GluA2–containing vesicles are preferentially targeted to the inner central region of the soma (Movie S5). Quantification of these observations, by counting the number of exocytic events along the long axis of the somatic region, confirmed that exocytic vesicles of pH-γ2S and tdt-GluA2 are spatially segregated on the somatic plasma membrane (Fig. 5 B–D). To rule out any potential artifacts of the fluorescent tags, we swapped the fluorescent tags on the two receptor subunits and imaged exocytosis of pH-GluA2 and tdt-γ2S. Exocytic events of these receptors displayed the same distributions as tdt-GluA2 and pH-γ2S, respectively (Fig. 5E). Exocytic events of pH-GluA2 and tdt-GluA2 occur with a similar inner central-somatic distribution (Fig. 5F), whereas exocytic events of pH-γ2S and tdt-γ2S have the same outer peripheral-somatic distribution (Fig. 5G). In addition, the distribution of pH-GluA2 exocytic events was not affected by the coexpression of other AMPA receptor subunits, such as GluA1 and GluA3 (Fig. S9 B–E). Overall, our observations suggest that the exocytic events of excitatory AMPA receptors and inhibitory GABA_A receptors are spatially segregated. The exocytosis of GluA2, a subunit present in most AMPA receptors, occurs at the inner region of the soma in contact with the coverslip, whereas the exocytosis of γ2S, a subunit present in most inhibitory GABA_A receptors, occurs at the outer region of the soma in contact with the coverslip.

Interestingly, this differential surface targeting of exocytosis of GluA2 and γ2S is regulated by Rab proteins. Whereas dominant negative Rab8 did not change the distribution of GluA2 exocytosis, which mostly occurs at the inner region of the somatic

membrane, the residual exocytic events of GluA2 after expression of dominant negative Rab4, Rab5, or Rab11 were distributed more evenly across the somatic membrane (Fig. 5H). The distribution of γ2S exocytosis was not affected by any of the Rab mutants (Fig. 5I). These data suggest that differential targeting of GluA2 and γ2S exocytosis on the plasma membrane potentially reflect specific exocytic pathways for each receptor. Although some GluA2-containing AMPA receptors can be delivered to the plasma membrane through the de novo exocytic pathway, the majority of AMPA receptors are delivered through recycling vesicles and inserted into the inner region of the soma in contact with the coverslip. However, most γ2S-containing GABA_A receptors are delivered to the plasma membrane through de novo exocytic vesicles, which specifically insert at the outer regions of the soma.

AMPA and GABA_A Receptors Exit the Golgi Apparatus As Different Vesicles. Because the constitutive exocytosis of both AMPA and GABA_A receptors seems to occur through a de novo exocytic pathway originating from the Golgi apparatus, we further asked whether the two receptor types are trafficked by different vesicles after they exit the Golgi. To image post-Golgi trafficking of receptors, we coexpressed EGFP- or tdTomato-tagged GluA2 and γ2S and then incubated transfected neurons at 20 °C to inhibit vesicle budding from the Golgi apparatus (42). Under this condition, we observed the accumulation of GluA2 and γ2S in the Golgi apparatus (Fig. S10A). After the 20 °C incubation, live neurons were imaged at 32 °C when post-Golgi trafficking is restored (43). We first examined whether the same receptor with different fluorescent tags is cotrafficked in the post-Golgi route by coexpressing EGFP-γ2S and tdt-γ2S, or EGFP-GluA2 and tdt-GluA2. We were able to visualize trafficking vesicles containing both EGFP-γ2S and tdt-γ2S (Fig. S10B and Movie S6), or both EGFP-GluA2 and tdt-GluA2 (Fig. S10C and Movie S6), indicating cotrafficking of these differentially tagged receptor subunits. However, we also observed many vesicles containing EGFP- or tdTomato-tagged subunits alone. This is likely due to the low number of receptors in each vesicle (Fig. S1 E–H) and the sensitivity of detection. In contrast, when we coexpressed EGFP-GluA2 and tdt-γ2S (Fig. 6A and Movie S7), or EGFP-γ2S and tdt-GluA2 (Fig. 6B and Movie S8), we very rarely observed the cotrafficking of GluA2 and γ2S. The percentage of cotrafficking events of different receptor pairs is significantly lower than that of same
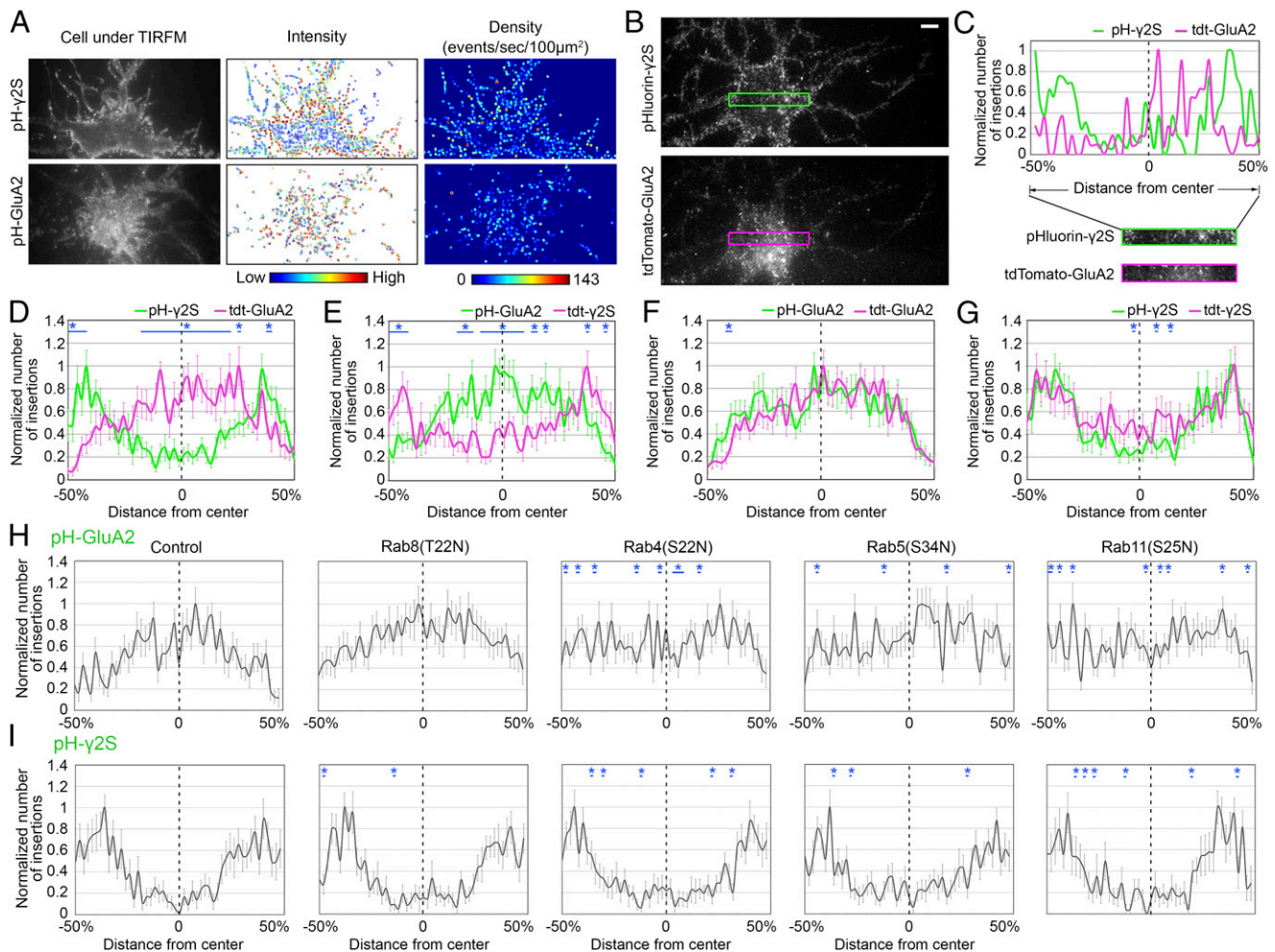
Gu et al.

www.manaraa.com

Fig. 5. GluA2 and γ2S are inserted into different domains of the somatic plasma membrane. (*A*) pH-γ2S and pH-GluA2 are inserted into different domains of the somatic plasma membrane. (*Left*) Neuron morphology under TIRFM. (*Middle*) Spatial location and intensity (shown in colors) of events for pH-GluA2 (*n* = 545) and pH-γ2S (*n* = 1,559) accumulating from 14 s. (*Right*) Heat map showing spatial density distributions of the events in the middle panel. Event density was calculated as the number of events per second per 100 μm² within a circular region (diameter: 0.48 μm). (*B*) Exocytosis of pH-γ2S and tdt-GluA2 in the same cell. Green and magenta rectangular regions represent the same somatic region for pH-γ2S and tdt-GluA2, respectively. (Scale bar: 5 μm.) (*C*) Quantification of exocytic events of pH-γ2S (green) and tdt-GluA2 (magenta) in the region shown in *B*. Normalized numbers of events along the long axis of the selected region were plotted against the distance from the center (maximal distances from the center on both directions were normalized as 50% and −50%). (*D–G*) Averaged distributions of exocytic events of pH-γ2S and tdt-GluA2 (*D*), pH-GluA2 and tdt-γ2S (*E*), pH-GluA2 and tdt-GluA2 (*F*), and pH-γ2S and tdt-γ2S (*G*). Green and magenta curves represent exocytic event of pH and tdt receptors, respectively. *n* = 13–17 for each group. (*H* and *I*) Effects of dominant negative Rabs on exocytic event distributions of GluA2 (*H*) and γ2S (*I*). Empty vector (−), Rab8(T22N), Rab4(S22N), Rab5(S34N), or Rab11(S25N) was coexpressed with pH receptors. *n* = 16–20 for each group. Asterisks indicate statistical significance compared with empty vector control.

receptor pairs (Fig. 6*C*), suggesting that vesicles exiting the Golgi carry preferentially GluA2 or γ2S alone. These results indicate that GluA2 and γ2S receptors are trafficked in separate vesicles after they exit the Golgi apparatus.

Endogenous AMPA and GABA_A Receptors Are Sorted into Different Vesicles. Our results in cultured hippocampal neurons strongly suggest that AMPA and GABA_A receptors are sorted into different intracellular vesicles before exocytosis. To further investigate whether endogenous receptors were also sorted into separate intracellular vesicular compartments in vivo we performed double-label immunogold EM studies in microsome-enriched fractions (P3) from adult rat brain. Rat brain homogenates were fractionated by differential centrifugation (44) and the fractions were characterized using markers of major intracellular organelles and vesicles (Fig. 7*A*). The P3 fraction contains membranes from the endoplasmic reticulum (ERP72, endoplasmic reticulum protein 72), lysosomes (LAMP1, lysosomal-associated

membrane protein 1), early endosomes (EEA1, early endosome antigen 1), recycling endosomes (synaxin13), and Golgi apparatus (TGN38, trans-Golgi network integral membrane protein 38). Other SNARE proteins, such as SNAP23, SNAP25, and VAMP2, were also present in the P3 fraction. Furthermore, GluA2 and γ2 are enriched in P3 fraction. The EM morphology of P3 fraction showed that the P3 pellet contained intact vesicular structures with different sizes (Fig. 7 *B* and *C*).

Double-immunogold labeling was performed on thin sections of the P3 pellet after a light fixation (Fig. 7*D*). The morphology of small intracellular trafficking vesicles, which are 50–300 nm in diameter (44), was largely preserved under this condition. GluA2 and γ2 were labeled by specific primary antibodies and secondary antibodies conjugated to 6-nm and 12-nm gold particles, respectively. The average number of 6-nm or 12-nm gold particles on each vesicle is two or three, respectively. The majority of vesicles (88%) contained only a single type of receptor whereas 12% of the vesicles contained both GluA2 and γ2. We observed that 37% of
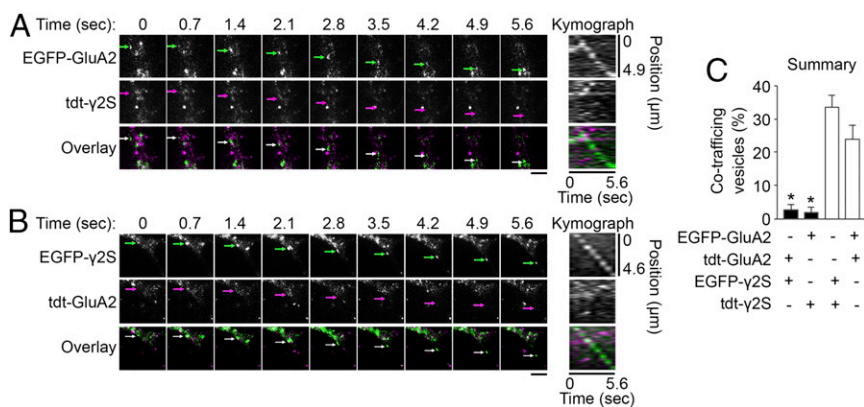
www.manaraa.com

Fig. 6. GluA2 and γ2S are trafficked in different vesicles when they exit the Golgi apparatus. (*A*) Time series of a post-Golgi trafficking vesicle containing only EGFP-GluA2, but not tdt-γ2S, as indicated by arrows at corresponding locations. (*Top*) EGFP-GluA2. (*Middle*) tdt-γ2S. (*Bottom*) Overlay of top and middle panels. (Scale bar: 2.5 μm.) The kymographs show the trafficking of the vesicle along its trajectory for EGFP-GluA2, tdt-γ2S and overlaid signal. (*B*) Time series of a post-Golgi trafficking vesicle containing only EGFP-γ2S, but not tdt-GluA2. (*C*) Quantification of cotrafficking events of EGFP- and tdt-tagged receptors after exit the Golgi apparatus. Asterisks indicate statistical significances.

the vesicles contained only GluA2, whereas 51% of the vesicles contained only γ2 (Fig. 7 *D* and *E*). Statistical analysis showed that GluA2 and γ2 are independently distributed on these vesicles without a significant colocalization ($P > 0.05$ compared with the null hypothesis that GluA2-containing vesicles and γ2-containing vesicles are independent vesicle populations; see *SI Materials and Methods* for details). Taken together, this in vivo result further supported the vesicular sorting model that AMPA and GABA$_A$ receptors are sorted into different intracellular trafficking vesicles before exocytosis.

Discussion

AMPA and GABA$_A$ receptors are selectively targeted to excitatory and inhibitory synapses (3), respectively. However, it is not clear when and how AMPA and GABA$_A$ receptors are sorted and trafficked into their target zones. To investigate this important question, we performed live TIRF imaging to directly visualize the constitutive exocytic vesicles of AMPA and GABA$_A$ receptors. In combination with immunocytochemistry, electrophysiology, and electron microscopy studies, we found that the exocytic sorting of these two receptor types follows the "vesicle sorting model" (Fig. 7*F*). AMPA and GABA$_A$ are initially sorted into different vesicles in the Golgi apparatus. The majority of GABA$_A$ receptors are directly delivered to the plasma membrane through the de novo

exocytic pathway under the regulation of Rab8. The SNAP23–syntaxin1–VAMP2 complex mediates the fusion of GABA$_A$ receptor-containing vesicle to the plasma membrane. However, exocytosis of AMPA receptors includes not only the Rab8-mediated de novo pathway but also the recycling pathway regulated by Rab4, 5, and 11. The fusion between AMPA receptor-containing vesicle and the plasma membrane is mediated by the SNAP25–syntaxin1–VAMP2 complex. In addition, we observed that vesicles containing AMPA receptors preferentially insert in the central region of the soma, whereas vesicles containing GABA$_A$ receptors preferentially insert in the periphery of the soma. This result was surprising and indicated that AMPA and GABA$_A$ receptors are not only differentially sorted into distinct vesicles but also targeted to distinct zones of the somatic plasma membrane during exocytosis.

This sorting of the major excitatory and inhibitory receptors in the somatodendritic region is reminiscent of the polarized trafficking of apical versus basolateral proteins in epithelial cells (45, 46) and somatodendritic versus axonal proteins in neurons (47, 48), which involves vesicular sorting in TGN and endosomes. Previous studies and our current research suggest a general strategy that proteins that function at different subdomains of the cell are sorted early into separate vesicle populations. This early sorting maximally ensures the independent targeting and regulation of each protein.
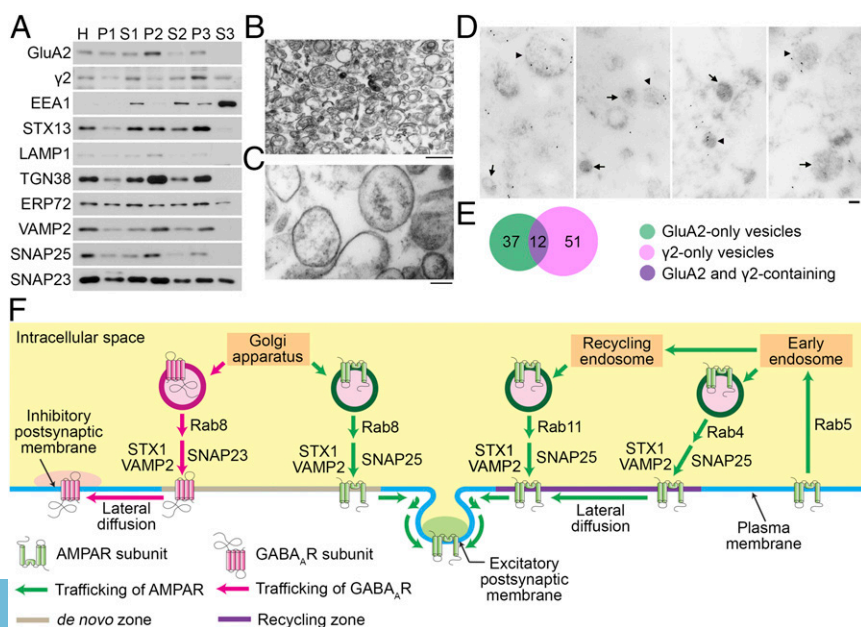

Fig. 7. Endogenous AMPA and GABA$_A$ receptors are sorted into different vesicles. (*A*) Subcellular fractionation of adult rat brain. Each fraction was normalized based on protein concentration. H, whole brain homogenate; P1, cell debris and nuclei; P2, washed synaptosomal fraction; P3, microsomal pellet; S1, postnuclear supernatant; S2, postsynaptosomal fraction; S3, soluble protein fraction. (*B* and *C*) Morphology of vesicles inP3 fraction under EM. (Scale bars: *B*, 500 nm; *C*, 100 nm.) (*D*) Double-immunogold EM of GluA2 and γ2 in P3 sections. GluA2 and γ2 were labeled by 6-nm (arrows) and 12-nm (arrow heads) immunogold beads, respectively. (Scale bar: 100 nm.) (*E*) Quantification of vesicles containing GluA2 or γ2 observed under double-immunogold EM. Green: GluA2-only vesicles (37% of all vesicles). Magenta: γ2-only vesicles (51%). Purple: GluA2 and γ2-containing vesicles (12%). n = 73. (*F*) Vesicular sorting model for constitutive exocytosis of AMPA and GABA$_A$ receptors.

Gu et al.

www.manaraa.com

Moreover, it is surprising that AMPA and GABA$_A$ receptors are delivered into distinct domains of the somatic membrane. Our data suggest the vesicles targeted at the central and peripheral regions of the soma originate from endocytic pathways and de novo exocytic pathways, respectively. This phenomenon indicates the presence of specialized zones on the plasma membrane for different exocytic pathways. Why would neurons deliver AMPA and GABA$_A$ receptors to different locations and through different pathways on the cell soma? In hippocampal neurons inhibitory synapses are often localized on proximal dendrites and the soma, whereas excitatory synapses are distributed both at proximal and distal dendrites (3, 49). The direct exocytosis of GABA$_A$ receptors to the peripheral somatic membrane would place the receptors near the location of inhibitory synapses. However, many AMPA receptors have to travel long distances to reach excitatory synapses on distal dendrites. The high level of constitutive exocytosis of AMPA receptors in the cell soma suggests that lateral diffusion of AMPA receptors from the somatic cell surface to proximal and possibly distal dendrites may play a significant role in maintaining surface and synaptic AMPA receptors. Consistent with this interpretation, a previous study had suggested that endogenous AMPA receptors are mostly exocytosed and recycled at extrasynaptic somatic sites (50). In addition, AMPA receptors may also be delivered through other trafficking pathways. For example, the transport of AMPA receptor-containing vesicles along microtubules certainly delivers AMPA receptors out to distal dendrites for local exocytosis into the extrasynaptic dendritic plasma membrane. It is possible that AMPA receptor containing recycling vesicles preferentially travel along microtubules assisting in the peripheral delivery of the receptors. Moreover, local translation of AMPA receptors subunits in dendrites will also likely play a role in the delivery of AMPA receptors to distal dendrites (1).

The constitutive exocytic events characterized here are distinct from previously reported activity-dependent AMPA receptors exocytic events from our laboratory and others (14, 15, 22). Those events for GluA1 and GluA2 homomers and heteromers are brighter and occur much less frequently and have slower kinetics (14, 15). The brighter, long-lasting GluA2 events are moderately regulated by neuronal activity and require the binding of NSF and RNA editing of Q/R site in GluA2 (15). The GluA1 events are significantly regulated by neuronal activity, as well as the binding of the 4.1N protein to GluA1 and by phosphorylation and palmitoylation of GluA1 (14). These brighter and slower events of pH-GluA1 contain around 50 receptor subunits (22). In contrast, we discovered constitutive exocytic events of GluA2 and γ2, which transiently occur at higher frequency and contain fewer than 10 receptor subunits per vesicle. These observations together suggest that activity-dependent and constitutive exocytic events originate from different vesicle populations with distinct properties. However, these two types of exocytosis share a common feature, which is that they both target extrasynaptic sites on the somatic membrane and dendritic shafts. Following the initial extrasynaptic exocytosis, the specialized synaptic clustering of AMPA and GABA$_A$ receptors is finally achieved by lateral diffusion of receptors from extrasynaptic pools to the synaptic membrane and stabilization of the receptors on specific postsynaptic membranes by scaffolding proteins (51). The exocytic events of GluA1 have been observed in spines when neuronal activity is stimulated (11, 52) but we and others have rarely observed spine exocytosis even in active neuronal cultures (10, 14, 15, 22).

The roles of SNARE complexes on constitutive trafficking or basal surface level of GABA$_A$ and AMPA receptors have been reported in many studies. However, the results are not fully consistent. In terms of GABA$_A$ receptor, slices from SNAP25 null animals showed an up-regulation of postsynaptic surface GABA$_A$ receptors (8), suggesting that SNAP25 is not necessary in GABA$_A$ receptor exocytosis and is in agreement with our results. Conversely, the surface and total levels of GABA$_A$ receptor α1 subunit

did not change in SNAP23$^{+/-}$ neurons (13). However, knockdown of SNAP23 by lentiviral-mediated shRNA expression only induced a modest reduction of surface AMPA receptors and no significant change of surface AMPA receptor levels was detected in SNAP23$^{+/-}$ mice (13), supporting our conclusion that SNAP23 is not required for AMPA receptor exocytosis. However, AMPA receptor surface level was not affected by knockdown of SNAP25 expression with lentiviral-mediated shRNA (13). No postsynaptic defects were detected after application of glutamate agonists in SNAP25-deficient neurons (53). In addition, it has been shown that Botox B rapidly reduced the amplitude of basal AMPA receptor-mediated EPSCs (7) and VAMP2 is required for constitutive delivery of AMPA receptors to the plasma membrane (16), consistent with our observation. In contrast, it has been shown that Botox B application had no effect on basal excitatory synaptic transmission (5). Tetanus toxin, which also cleaves VAMP2 and other Botox B-sensitive VAMPs (19), did not change amplitude of basal AMPA mEPSCs (6). What could be responsible for these contradictory results? First, most previous studies have not directly measured exocytic events. The surface receptor levels or synaptic current amplitude reflect the effects of multiple trafficking steps, including receptor exocytosis, endocytosis, lateral diffusion, and stabilization. So, it is critical to investigate roles of a certain molecule while isolating a particular trafficking event, as we have done here using TIRFM to specifically isolate exocytosis. Second, perturbation of trafficking events by genetic ablation and lentiviral-mediated knockdown of particular genes could induce compensatory expression of other mechanistically related proteins. For this reason, we have used acute neurotoxin treatments and short-term shRNA-mediated knockdown to complement each other. Third, it has been shown that surface levels of postsynaptic receptors, especially AMPA receptors, are regulated by long-lasting homeostatic changes in global neuronal activity, so called "synaptic scaling" (54). SNARE complexes are critical for presynaptic neurotransmitter release (55), and knockdown of particular SNARE components by genetic or virus-based shRNA approaches could possibly modulate neuronal activity in the whole preparation and indirectly affect postsynaptic receptors. Therefore, disruption of SNARE proteins at the single-cell level by sparse transfection of shRNAs, as we have done here, is more reliable when studying SNARE function in postsynaptic receptor trafficking to demonstrate that effects are cell-autonomous and independent of network activity.

In summary, by directly studying the constitutive exocytosis of AMPA and GABA$_A$ receptors, we found that the segregation of AMPA and GABA$_A$ receptors occurs early during intracellular vesicle trafficking. AMPA or GABA$_A$ receptor-containing vesicles are sorted in the Golgi and exit via distinct exocytic vesicles. AMPA receptors are highly targeted to recycling pathways, whereas GABA$_A$ receptors are not. Moreover, these distinct exocytic events occur in different regions of the cell surface. AMPA and GABA$_A$ receptor exocytic events share certain properties but are also distinct in several aspects and are differentially regulated by specific SNARE complexes and Rab proteins. These results demonstrate the neuron's capacity to elaborately sort different postsynaptic receptors to regulate excitatory and inhibitory transmission.

Methods

Animal Use. All animal experiments were performed with approval by the Animal Care and Use Committee at Johns Hopkins University School of Medicine.

Fusion Constructs. pHluorin-, EGFP-, and tdTomato-GluA2 were constructed in pcDNA3.1 hygro- vector by inserting the fluorescent proteins between Asn25 and Ser26 amino acids of rat GluA2 (flip). pHluorin-, EGFP-, and tdTomato-γ2S were constructed in pcDNA3.1 hygro- vector by inserting the fluorescent proteins between Asp42 and Asp43 amino acids of mouse γ2S.

Dual-TIRFM Imaging. An Olympus IX71 microscope with a plan-Apo objective (100×, N.A. 1.45, oil; Olympus) was used for dual-TIRFM imaging with 488-nm and 568-nm excitation lasers. See *SI Materials and Methods* for extended details.

www.manaraa.com

1. Shepherd JD, Huganir RL (2007) The cell biology of synaptic plasticity: AMPA receptor trafficking. *Annu Rev Cell Dev Biol* 23:613–643.
2. Jacob TC, Moss SJ, Jurd R (2008) GABA(A) receptor trafficking and its role in the dynamic modulation of neuronal inhibition. *Nat Rev Neurosci* 9(5):331–343.
3. Craig AM, Blackstone CD, Huganir RL, Banker G (1994) Selective clustering of glutamate and gamma-aminobutyric acid receptors opposite terminals releasing the corresponding neurotransmitters. *Proc Natl Acad Sci USA* 91(26):12373–12377.
4. Maletic-Savatic M, Koothan T, Malinow R (1998) Calcium-evoked dendritic exocytosis in cultured hippocampal neurons. Part II: Mediation by calcium/calmodulin-dependent protein kinase II. *J Neurosci* 18(17):6814–6821.
5. Lledo PM, Zhang X, Südhof TC, Malenka RC, Nicoll RA (1998) Postsynaptic membrane fusion and long-term potentiation. *Science* 279(5349):399–403.
6. Lu W, et al. (2001) Activation of synaptic NMDA receptors induces membrane insertion of new AMPA receptors and LTP in cultured hippocampal neurons. *Neuron* 29(1):243–254.
7. Lüscher C, et al. (1999) Role of AMPA receptor cycling in synaptic transmission and plasticity. *Neuron* 24(3):649–658.
8. Tafoya LC, et al. (2006) Expression and function of SNAP-25 as a universal SNARE component in GABAergic neurons. *J Neurosci* 26(30):7826–7838.
9. Kopec CD, Real E, Kessels HW, Malinow R (2007) GluR1 links structural and functional plasticity at excitatory synapses. *J Neurosci* 27(50):13706–13718.
10. Makino H, Malinow R (2009) AMPA receptor incorporation into synapses during LTP: The role of lateral movement and exocytosis. *Neuron* 64(3):381–390.
11. Kennedy MJ, Davison IG, Robinson CG, Ehlers MD (2010) Syntaxin-4 defines a domain for activity-dependent exocytosis in dendritic spines. *Cell* 141(3):524–535.
12. Park M, Penick EC, Edwards JG, Kauer JA, Ehlers MD (2004) Recycling endosomes supply AMPA receptors for LTP. *Science* 305(5692):1972–1975.
13. Suh YH, et al. (2010) A neuronal role for SNAP-23 in postsynaptic glutamate receptor trafficking. *Nat Neurosci* 13(3):338–343.
14. Lin DT, et al. (2009) Regulation of AMPA receptor extrasynaptic insertion by 4.1N, phosphorylation and palmitoylation. *Nat Neurosci* 12(7):879–887.
15. Araki Y, Lin DT, Huganir RL (2010) Plasma membrane insertion of the AMPA receptor GluA2 subunit is regulated by NSF binding and Q/R editing of the ion pore. *Proc Natl Acad Sci USA* 107(24):11080–11085.
16. Jurado S, et al. (2013) LTP requires a unique postsynaptic SNARE fusion machinery. *Neuron* 77(3):542–558.
17. Arendt KL, et al. (2015) Retinoic acid and LTP recruit postsynaptic AMPA receptors using distinct SNARE-dependent mechanisms. *Neuron* 86(2):442–456.
18. Südhof TC, Rothman JE (2009) Membrane fusion: Grappling with SNARE and SM proteins. *Science* 323(5913):474–477.
19. Schiavo G, Matteoli M, Montecucco C (2000) Neurotoxins affecting neuroexocytosis. *Physiol Rev* 80(2):717–766.
20. Axelrod D (2001) Total internal reflection fluorescence microscopy in cell biology. *Traffic* 2(11):764–774.
21. Miesenböck G, De Angelis DA, Rothman JE (1998) Visualizing secretion and synaptic transmission with pH-sensitive green fluorescent proteins. *Nature* 394(6689):192–195.
22. Yudowski GA, et al. (2007) Real-time imaging of discrete exocytic events mediating surface delivery of AMPA receptors. *J Neurosci* 27(41):11112–11121.
23. Jacob TC, et al. (2005) Gephyrin regulates the cell surface dynamics of synaptic GABAA receptors. *J Neurosci* 25(45):10469–10478.
24. Sankaranarayanan S, De Angelis D, Rothman JE, Ryan TA (2000) The use of pHluorins for optical measurements of presynaptic activity. *Biophys J* 79(4):2199–2208.
25. Shaner NC, et al. (2004) Improved monomeric red, orange and yellow fluorescent proteins derived from Discosoma sp. red fluorescent protein. *Nat Biotechnol* 22(12):1567–1572.
26. Shaner NC, Steinbach PA, Tsien RY (2005) A guide to choosing fluorescent proteins. *Nat Methods* 2(12):905–909.
27. Wu LG, Hamid E, Shin W, Chiang HC (2014) Exocytosis and endocytosis: Modes, functions, and coupling mechanisms. *Annu Rev Physiol* 76:301–331.
28. Hayashi T, et al. (1994) Synaptic vesicle membrane fusion complex: Action of clostridial neurotoxins on assembly. *EMBO J* 13(21):5051–5061.
29. Verderio C, et al. (2006) Entering neurons: Botulinum toxins and synaptic vesicle recycling. *EMBO Rep* 7(10):995–999.
30. Washbourne P, Liu XB, Jones EG, McAllister AK (2004) Cycling of NMDA receptors during trafficking in neurons before synapse formation. *J Neurosci* 24(38):8253–8264.
31. Pan PY, et al. (2005) SNAP-29-mediated modulation of synaptic transmission in cultured hippocampal neurons. *J Biol Chem* 280(27):25769–25779.
32. Su Q, Mochida S, Tian JH, Mehta R, Sheng ZH (2001) SNAP-29: A general SNARE protein that inhibits SNARE disassembly and is implicated in synaptic transmission. *Proc Natl Acad Sci USA* 98(24):14038–14043.
33. Teng FY, Wang Y, Tang BL (2001) The syntaxins. *Genome Biol* 2(11)REVIEWS3012.
34. Schiavo G, Shone CC, Bennett MK, Scheller RH, Montecucco C (1995) Botulinum neurotoxin type C cleaves a single Lys-Ala bond within the carboxyl-terminal region of syntaxins. *J Biol Chem* 270(18):10566–10570.
35. Araki S, et al. (1997) Inhibition of the binding of SNAP-23 to syntaxin 4 by Munc18c. *Biochem Biophys Res Commun* 234(1):257–262.
36. Chen D, Minger SL, Honer WG, Whiteheart SW (1999) Organization of the secretory machinery in the rodent brain: Distribution of the t-SNAREs, SNAP-25 and SNAP-23. *Brain Res* 831(1-2):11–24.
37. Pevsner J, et al. (1994) Specificity and regulation of a synaptic vesicle docking complex. *Neuron* 13(2):353–361.
38. Trimble WS, Cowan DM, Scheller RH (1988) VAMP-1: A synaptic vesicle-associated integral membrane protein. *Proc Natl Acad Sci USA* 85(12):4538–4542.
39. Baumert M, Maycox PR, Navone F, De Camilli P, Jahn R (1989) Synaptobrevin: An integral membrane protein of 18,000 daltons present in small synaptic vesicles of rat brain. *EMBO J* 8(2):379–384.
40. Trimble WS, Gray TS, Elferink LA, Wilson MC, Scheller RH (1990) Distinct patterns of expression of two VAMP genes within the rat brain. *J Neurosci* 10(4):1380–1387.
41. Stenmark H (2009) Rab GTPases as coordinators of vesicle traffic. *Nat Rev Mol Cell Biol* 10(8):513–525.
42. Matlin KS, Simons K (1983) Reduced temperature prevents transfer of a membrane glycoprotein to the cell surface but does not prevent terminal glycosylation. *Cell* 34(1):233–243.
43. Yeaman C, et al. (2004) Protein kinase D regulates basolateral membrane protein exit from trans-Golgi network. *Nat Cell Biol* 6(2):106–112.
44. Lee SH, Valtschanoff JG, Kharazia VN, Weinberg R, Sheng M (2001) Biochemical and morphological characterization of an intracellular membrane compartment containing AMPA receptors. *Neuropharmacology* 41(6):680–692.
45. Carmosino M, Valenti G, Caplan M, Svelto M (2010) Polarized traffic towards the cell surface: How to find the route. *Biol Cell* 102(2):75–91.
46. Rodriguez-Boulan E, Kreitzer G, Müsch A (2005) Organization of vesicular trafficking in epithelia. *Nat Rev Mol Cell Biol* 6(3):233–247.
47. Lai HC, Jan LY (2006) The distribution and targeting of neuronal voltage-gated ion channels. *Nat Rev Neurosci* 7(7):548–562.
48. Kennedy MJ, Ehlers MD (2006) Organelles and trafficking machinery for postsynaptic plasticity. *Annu Rev Neurosci* 29:325–362.
49. Megías M, Emri Z, Freund TF, Gulyás AI (2001) Total number and distribution of inhibitory and excitatory synapses on hippocampal CA1 pyramidal cells. *Neuroscience* 102(3):527–540.
50. Adesnik H, Nicoll RA, England PM (2005) Photoinactivation of native AMPA receptors reveals their real-time trafficking. *Neuron* 48(6):977–985.
51. Opazo P, Choquet D (2011) A three-step model for the synaptic recruitment of AMPA receptors. *Mol Cell Neurosci* 46(1):1–8.
52. Patterson MA, Szatmari EM, Yasuda R (2010) AMPA receptors are exocytosed in stimulated spines and adjacent dendrites in a Ras-ERK-dependent manner during long-term potentiation. *Proc Natl Acad Sci USA* 107(36):15951–15956.
53. Washbourne P, et al. (2002) Genetic ablation of the t-SNARE SNAP-25 distinguishes mechanisms of neuroexocytosis. *Nat Neurosci* 5(1):19–26.
54. Turrigiano GG (2008) The self-tuning neuron: Synaptic scaling of excitatory synapses. *Cell* 135(3):422–435.
55. Lin RC, Scheller RH (2000) Mechanisms of synaptic vesicle exocytosis. *Annu Rev Cell Dev Biol* 16:19–49.
56. Fu J, Naren AP, Gao X, Ahmmed GU, Malik AB (2005) Protease-activated receptor-1 activation of endothelial cells induces protein kinase Calpha-dependent phosphorylation of syntaxin 4 and Munc18c: Role in signaling p-selectin expression. *J Biol Chem* 280(5):3178–3184.
57. Wu PH, Arce SH, Burney PR, Tseng Y (2009) A novel approach to high accuracy of video-based microrheology. *Biophys J* 96(12):5103–5111.
58. Wu PH, et al. (2012) High-throughput ballistic injection nanorheology to measure cell mechanics. *Nat Protoc* 7(1):155–170.

Gu et al.

www.manaraa.com